

ESI for: Length-scale Dependent Transport Properties of Colloidal and Protein Solutions for Prediction of Crystal Nucleation Rates

Tomasz Kalwarczyk,^{*a} Krzysztof Sozański,^a Sławomir Jakiela,^a Agnieszka Wiśniewska,^a Ewelina Kalwarczyk,^a Katarzyna Kryszczuk,^a Sen Hou,^{a,b} and Robert Holyst^{*a}

Experimental part

Measurements of macroscopic viscosity of protein solutions

We measured the relative viscosity η_r of BSA and lysozyme solutions at pH=4.7 and at pH=7.0, respectively. Ionic strength of the solutions of both proteins was kept at the level of I=154 mM. We used a custom designed steel capillary viscometer consisting of a small syringe (5 ml, Polfa, Poland) and a two-meter thin capillary (I.D. 205 μm , Mifam, Poland) connecting the syringe with a collecting vessel placed on a balance (Radwag, XA/2X). The syringe was pressurized by an outer compressor using a manual pressure regulator. Custom-written software (LabWindows/CVI) allowed us to record weight changes of the collecting vessel. We measured the flow times of given fluid and reference fluid with known viscosity – water (Millipore, viscosity $\eta_0 = 0.890 \text{ mPa}\cdot\text{s}$, density $\rho_{\text{H}_2\text{O}} = 997 \text{ kg}\cdot\text{m}^{-3}$). The temperature of the whole system was stabilized by a styrofoam box. The viscosity of a given fluid was calculated on the basis of equation: $\eta_m/\eta_0 = \rho t / (\rho_{\text{H}_2\text{O}} t_{\text{H}_2\text{O}})$ where η_m - viscosity, ρ - density and t - flow time (the H_2O index relates to the reference fluid – water). The maximum relative error of measured fluid viscosity was 0.5 %.

Measurements of diffusion in protein solutions

Self diffusion of proteins was measured using fluorescence correlation spectroscopy (FCS) technique. The experimental setup was based on a Nikon C1 inverted confocal microscope, equipped with a water immersion objective, Nikon PlanApo 60x (NA=1.20). The complete system for time-correlated single photon counting as well as software for raw data analysis was provided by PicoQuant GmbH (Germany). A 488 nm pulse diode laser was used for excitation of fluorescently labelled proteins. The temperature control was realized by means of an Okolab H201 cage incubator. During each measurement, at least 15 independent FCS curves were recorded, with acquisition time for each curve between 30 and 90 s, depending on the fluorescence intensity and other experimental parameters. The data was combined to perform a cumulative analysis and fitting (using simple models, which assumed Gaussian shape of the detection volume).

ζ -potential measurements

We performed ζ -potential measurements using a Zetasizer Nano ZS apparatus (Malvern Instruments Ltd.). The measurements were carried out in disposable folded capillary zeta cells, using approximately 1 ml of solution per measurement. In order to obtain desired temperature each sample was incubated for 2 minutes. The data was analysed using the Smolu-

chowski approximation. All the mentioned measurements, irrespectively on the method, were performed at 25 °C.

Analysis

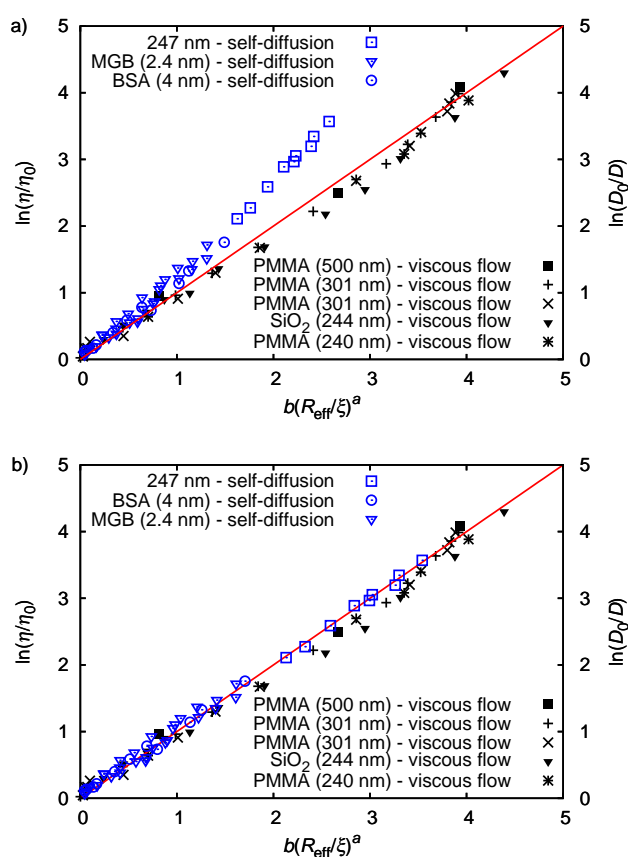


Fig. S1 Scaling plot of the relative viscosity and the reciprocal of the relative diffusion coefficient. Figure a) shows literature¹⁻³ data for macroscopic viscosity of hard-sphere solutions and the self-diffusion data for PMMA particles ($r_p = 247 \text{ nm}$)¹ and for proteins: bovine serum albumin (BSA, $r_p = 4 \text{ nm}$)⁴, and myoglobin (MGB, $r_p = 2.4 \text{ nm}$)⁴. Discrepancies between data for self-diffusion and for viscous flow are due to the caging/depletion effect. Introducing $d = 1 + (2.02 \pm 0.08) \psi/\psi_{\text{tcp}}$ into R_{eff} (cf. Equation 3 from the Main Text) results in the same scaling of both self-diffusion as well as viscosity data, as depicted in Figure b). In both plots solid red line represents a linear curve with slope equal to 1.

Functional forms describing the viscosity/diffusion in a dense colloidal solutions

Viscosity of dense hard-sphere solutions and the process of diffusion occurring in those solutions are, in the literature, de-

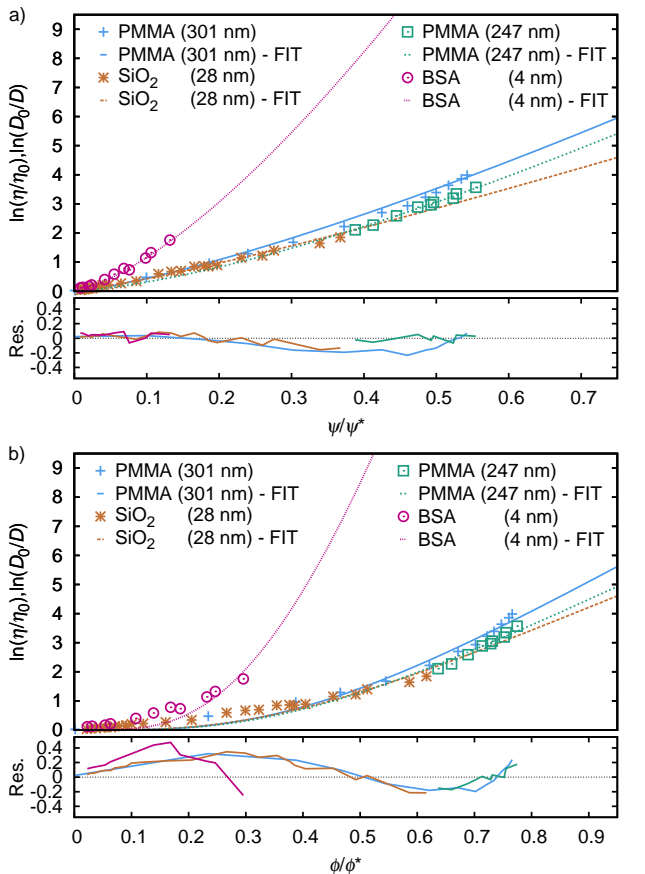


Fig. S2 The logarithm of the relative viscosity or of the reciprocal of the relative diffusion coefficient. Figure **a**) shows literature data for macroscopic viscosity of colloidal solutions consisting of PMMA hard-sphere like particles of $r_p = 301 \text{ nm}^1$, polydisperse SiO_2 hard-sphere like particles of $r_p = 28 \text{ nm}^1$. Plot shows also the data for self-diffusion of PMMA particles ($r_p = 247 \text{ nm}^1$) and for proteins: bovine serum albumin (BSA, $r_p = 4 \text{ nm}^4$). Curves represent least square fitting of scaling equation (equations 1) with ξ and R_{eff} given by equations 3 and 4 respectively. Bottom plot represents residue plot being the difference of the data and the fit. Figure **b**) shows the same set of data as in panel **a**). Curves represent least square fit of the scaling equation (Equation 1) to the data with R_{eff} given by equation 4 but with ψ and ψ_{rcp} replaced with ϕ and ϕ_{rcp} , respectively. For this plot we obtained a new set of parameters $a_\phi = 4.2 \pm 0.5$ and $d_\phi = 2.17 \pm 0.01$ and $b_\phi = 1.9 \pm 0.1$ for monodisperse hard-sphere, $b_\phi = 1.64 \pm 0.01$ for polydisperse hard-sphere, and $b_\phi = 14.3 \pm 0.4$ for BSA. Above parameters we calculate in the same manner as described in the main text. Comparison of residues clearly shows that model including ψ dependence describes the data reasonably good when compared with only ϕ dependence.

scribed by different functional forms. For example, the viscosity of hard-sphere suspensions is usually described (following Hunter and Weeks⁷) by the Doolittle equation

$$\eta_r = C_1 \exp \left[\frac{C_2 \phi}{\phi_{\text{rcp}} - \phi} \right] \quad (\text{S1})$$

with C_1 and C_2 being free parameters. The short-time diffusion coefficient is on the other hand given by equation (S2),

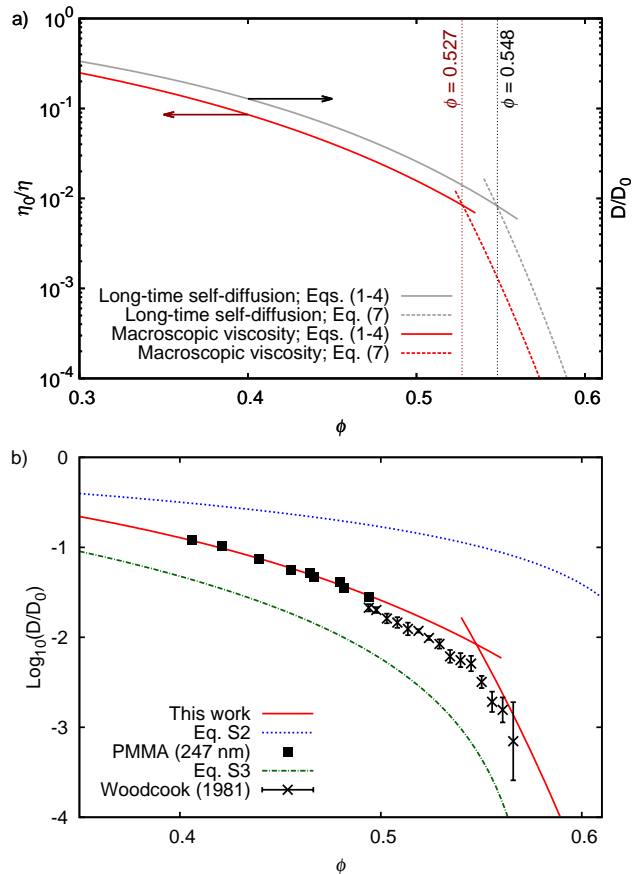


Fig. S3 Panel **a**) shows reciprocal of the macroscopic viscosity of the hard-sphere solution related to the viscosity of the solvent (left y-axis) and relative self-diffusion coefficient of the particle in hard-sphere solution (right y-axis); both as a function of the volume fraction ϕ of suspended particles. Below a certain volume fraction, $\phi = 0.527$ for viscosity and $\phi = 0.548$ for diffusion, both viscosity and diffusion are described by Eqs. (1-4) while above those ϕ viscosity and diffusion are described by Eq. (7). Panel **b**) shows comparison between the short- and long-time self-diffusion coefficient in concentrated suspensions of hard-spheres. We calculate the long-time self-diffusion coefficient using our scaling formulae. Following the works of Auer and Frenkel⁵ we calculate the short-time self-diffusion coefficient using relation (S2). Green, dashed-dotted line correspond to the long-time diffusion coefficient calculated with equation (S3). Square points correspond to the experimental values of the long-time self-diffusion coefficients of PMMA particles¹ while crosses correspond to the data of Woodcock⁶ who performed molecular dynamics simulations.

whereas the long-time self-diffusion by equation (S3).

$$\frac{D_S}{D_0} = \left(1 - \frac{\phi}{0.64} \right)^\delta \quad (\text{S2})$$

$$\frac{D_L}{D_0} = \left(1 - \frac{\phi}{0.58} \right)^\delta \quad (\text{S3})$$

Here δ is a free parameter equal to 1.17 for the short-time self-diffusion coefficient and varying from 1.74 (cf. reference 8) to 2.6 for the long-time self-diffusion coefficient (see references 9, 10, and 11).

In principle when the fluctuation-dissipation theorem

(FDT) is fulfilled in a given system the ratio of the relative viscosity η/η_0 should be equal to the reciprocal of the relative long-time diffusion coefficient D_0/D_L . At first look equations (S1) and (S3) do not allow for exhibit equality due to a different ϕ -dependence. Equations (1-4) from the main text, however provides a unified description of the viscosity and the long-time diffusion validating the FDT.

Equation (S3) with $\delta \approx 2.6$ was used to describe the long-time diffusion for calculations of the nucleation rates in both simulation and experimental studies. Filion and co-workers¹¹ used it to expressed the nucleation rate in terms of the long-time diffusion coefficient. Harland and van Megen used equation (S3) to fit their experimental data using the classical nucleation theory. Their expression for I^* required scaling by the free parameter equal to 0.01. Indeed the expression (S3) gives values about two orders of magnitude lower than the values for experimental or simulated data on long-time diffusion as presented in figure S3.

Comparison of the method with the classical nucleation theory We compare our results with the nucleation rates calculated from combination of our scaling equation with the classical nucleation theory where equation (S4) is used to calculate the nucleation barrier.

$$P = \exp \left[-\frac{4\pi^3\gamma^3}{27\phi_s^2\Delta\mu^2} \right] \quad (\text{S4})$$

where γ is a surface tension at the liquid-solid interface. ϕ_s and $\Delta\mu$ are the volume fraction of solids and the chemical potential difference between the solid phase and the metastable phase and both are expressed by the quadratic approximations (following Sinn *et al.*¹⁰):

$$\phi_s = 0.5455 + 1.308(\phi - \phi_F) - 2.93(\phi - \phi_F)^2 \quad (\text{S5})$$

$$\Delta\mu = -10.354(\phi - \phi_F) - 56.23(\phi - \phi_F)^2 \quad (\text{S6})$$

where ϕ_F is a volume fraction at the freezing point and is equal to 0.494. Figure S4 shows comparison of the simulated, predicted and experimental data with our calculations using CNT (eq. (S4)).

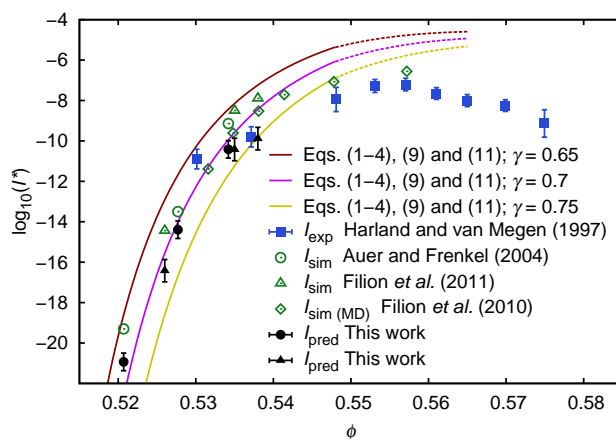


Fig. S4 Comparison of the experimental, calculated, and simulated nucleation rates with the values calculated from the classical nucleation theory according to equation (S4). We calculated the nucleation rates for different values of the surface tension γ (following Auer and Frenkel⁵). Irrespectively on the value of γ we obtained overestimated values of I^* with respect to the experimental and simulated values of I^* . Curves representing CNT calculations were plotted in the range of volume fractions for which our model described the data for diffusion (cf. figure S3b). Symbols the same as in figure 4 from the main text.

References

- 1 P. N. Segre, S. P. Meeker, P. N. Pusey and W. C. K. Poon, *Phys. Rev. Lett.*, 1995, **75**, 958.
- 2 S. P. Meeker, W. C. K. Poon and P. N. Pusey, *Phys. Rev. E*, 1997, **55**, 5718.
- 3 Z. Cheng, J. Zhu, P. M. Chaikin, S.-E. Phan and W. B. Russel, *Phys. Rev. E*, 2002, **65**, 041405.
- 4 I. V. Nesmelova, V. D. Skirda and V. D. Fedotov, *Biopolymers*, 2002, **63**, 132–140.
- 5 S. Auer and D. Frenkel, *Nature*, 2001, **409**, 1020–1023.
- 6 L. V. Woodcock, *Annals of the New York Academy of Sciences*, 1981, **371**, 274–298.
- 7 G. L. Hunter and E. R. Weeks, *Reports on Progress in Physics*, 2012, **75**, 066501.
- 8 J. Duijneveldt and H. Lekkerkerker, in *Science and Technology of Crystal Growth*, ed. J. Eerden and O. Bruinsma, Springer Netherlands, 1995, pp. 279–290.
- 9 J. L. Harland and W. van Megen, *Phys. Rev. E*, 1997, **55**, 3054.
- 10 C. Sinn, A. Heymann, A. Stipp and T. Palberg, in *Trends in Colloid and Interface Science XV*, Springer, 2001, pp. 266–275.
- 11 L. Filion, M. Hermes, R. Ni and M. Dijkstra, *The Journal of chemical physics*, 2010, **133**, 244115.